

## New deformed model of $\alpha$ -decay half-lives with a microscopic potential

Chang Xu<sup>1</sup> and Zhongzhou Ren<sup>1,2,3,\*</sup>

<sup>1</sup>Department of Physics, Nanjing University, Nanjing 210008, China

<sup>2</sup>Center of Theoretical Nuclear Physics, National Laboratory of Heavy-Ion Accelerator, Lanzhou 730000, China

<sup>3</sup>CPNPC, Nanjing University, Nanjing 210008, China

(Received 19 January 2006; published 6 April 2006)

The  $\alpha$ -decay half-lives of deformed nuclei are investigated in a new version of the density-dependent cluster model. By the multipole expansion method, the deformation- and orientation-dependent double-folding potential is derived to calculate the  $\alpha$ -decay width through a deformed Coulomb barrier. We perform systematic calculations for the ground-state  $\alpha$  transitions of even-even nuclei with  $Z = 52-104$ . The theoretical results are in good agreement with the experimental data. This is, to our knowledge, the first deformed calculation of  $\alpha$ -decay half-lives within the framework of microscopic double-folding potentials. A unified description of  $\alpha$ -decay half-lives of both spherical and deformed nuclei is obtained by the microscopic potentials.

DOI: 10.1103/PhysRevC.73.041301

PACS number(s): 23.60.+e, 21.10.Tg, 21.60.-n, 24.10.-i

One of the most important decay modes for unstable medium and heavy nuclei is  $\alpha$  radioactivity, which is a quantum-tunneling effect [1–19]. One usually simplifies the calculations of  $\alpha$ -decay half-lives by assuming a spherical shape for nuclei. This approximation is reasonable because most of the ground-state  $\alpha$  emitters are spherical or moderate deformed [20,21]. Various spherical calculations with different potentials gave similar results of half-lives [11–13,15]. The available experimental half-lives of  $\alpha$  decay can generally be reproduced within a factor of 3–4 by spherical calculations [15,17]. Although this agreement between experiment and theory is satisfactory, the results of the spherical model can be further improved by taking into account the influence of nuclear deformations [5,6,18,19], not only for pursuing a better agreement but also for obtaining a more microscopic understanding of  $\alpha$  decay.

The aim of this communication is to study the  $\alpha$ -decay half-lives of deformed even-even  $\alpha$  emitters in a new version of the density-dependent cluster model (DDCM). The microscopic-deformation- and orientation-dependent  $\alpha$ -core potentials are evaluated from the well-established double-folding model by the multipole expansion method [22–26]. This is a novel development of the spherical DDCM [16,17] because the double-folding potentials between a spherical-deformed pair of nuclei are difficult to calculate, and such potentials have rarely been used in the calculations of  $\alpha$  decays. To extend the model from the spherical case to a deformed one also involves complicated derivations of formulas and a large increase of time of numerical computation in computers. This is well known in both the model of a nuclear structure and the model of a nuclear reaction. Therefore it is interesting to see how the occurrence of a spheroidal deformation affects the microscopic  $\alpha$ -core potentials and the corresponding  $\alpha$ -decay width. Here we present a new deformed model of nonspherical  $\alpha$ -decay half-lives by using microscopic double-folding potentials. The previous research on  $\alpha$ -decay half-lives of deformed nuclei

was based on deformed potentials such as a square potential or a Woods-Saxon potential [5,18,19]. The double-folding potential is based on the popular M3Y potential, which is from the fitting of a  $G$  matrix of the Reid potential [16,17,22–26]. Therefore the deformed version of the DDCM with microscopic double-folding potentials is well grounded in physics.

We assume that a spherical  $\alpha$  particle interacts with a deformed daughter nucleus that has an axially symmetric deformation. The total  $\alpha$ -core potential is a sum of nuclear potential, the Coulomb potential, and the centrifugal potential [17]:

$$V_{\text{Total}}(R, \beta) = V_N(R, \beta) + V_C(R, \beta) + \frac{\hbar^2 (L + \frac{1}{2})^2}{2\mu R^2}, \quad (1)$$

where  $R$  is the separation between the mass center of the  $\alpha$  particle and the mass center of the core and  $\beta$  is the orientation angle of the  $\alpha$  particle with respect to the symmetry axis of the daughter nucleus. The nuclear and Coulomb potentials from the double-folding procedure are given by [22,23]

$$V_{N \text{ or } C}(R, \beta) = \int d\mathbf{r}_1 d\mathbf{r}_2 \rho_1(\mathbf{r}_1) \rho_2(\mathbf{r}_2) v(\mathbf{s}). \quad (2)$$

Here the quantity  $|\mathbf{s}|$  is the distance between a nucleon in the core and a nucleon in the  $\alpha$  particle;  $\mathbf{s} = \mathbf{R} + \mathbf{r}_2 - \mathbf{r}_1$  [23]. The density distribution of the spherical  $\alpha$  particle is a standard Gaussian form given by Satchler and Love [23]. In the spherical version of the DDCM [17], the density distribution of the daughter nucleus is from the standard Fermi distribution of electron scattering and the parameters are from standard textbooks [27–29]. Here the nuclear deformation is included, and the density distribution of the deformed daughter nucleus is a natural extension to the spherical one:

$$\rho_2(r_2, \theta) = \rho_0 / (1 + \exp\{[r_2 - R(\theta)]/a\}), \quad (3)$$

where the value of  $\rho_0$  is fixed by integration of the density distribution equivalent to the mass number of daughter nucleus  $A_d$ . The half-density radius  $R(\theta)$  is given by  $R(\theta) = R_0[1 + \beta_2 Y_{20}(\theta) + \beta_4 Y_{40}(\theta)]$ . The constants  $R_0 = 1.07 A_d^{1/3}$  fm

\*Electronic address: zren@nju.edu.cn

and  $a = 0.54$  fm are taken from Refs. [27–29]. When  $\beta_2 = \beta_4 = 0$ , the matter radius of heavy nuclei with this choice is  $R_{\text{rms}} \approx 1.2 \times A^{1/3}$  (fm), and this goes back to spherical case automatically [27–29]. Because the density distribution of the daughter nucleus is deformed, Eq. (2) involves a complex six-dimensional integral [22,23]. Thus the derivation of double-folding potentials becomes rather difficult for the spherical-deformed interacting pair [24,25]. In our calculations, we solve the double-folding potential numerically by using the multipole expansion method [24,25]. In the multipole expansion, the density distribution of daughter nucleus is expanded as [24]

$$\rho(r, \theta) = \sum_{l=0,2,4,\dots} \rho_l(r) Y_{l0}(\theta), \quad (4)$$

and the corresponding intrinsic form factor has the form [24]

$$\tilde{\rho}^{(l)}(k) = \int_0^\infty dr r^2 \rho_l(r) j_l(kr). \quad (5)$$

The double-folding potential can then be evaluated by a sum of different multipole components [24]:

$$V_{N \text{ or } C}(R, \beta) = \sum_{l=0,2,4,\dots} V_{N \text{ or } C}^l(R, \beta), \quad (6)$$

with

$$V_{N \text{ or } C}^l(R, \beta) = (2/\pi) [(2l+1)/4\pi]^{1/2} \times \int_0^\infty dk k^2 j_l(kR) \tilde{\rho}_1(k) \tilde{\rho}_2^{(l)}(k) \tilde{v}(k) P_l(\cos \beta), \quad (7)$$

where  $\tilde{\rho}_1(k)$  is the Fourier transformation of the density distribution of the  $\alpha$  particle,  $\tilde{\rho}_2^{(l)}(k)$  is the intrinsic form factor of daughter nucleus,  $\tilde{v}(k)$  is the Fourier transformation of a local two-body effective interaction, and  $P_l(\cos \beta)$  is the Legendre function of degree  $l$ . In our calculations, we use the famous M3Y-Reid-type nucleon-nucleon interaction and the standard proton-proton Coulomb interaction [22,23,26]. The M3Y interaction proposed by Bertsch *et al.* [22] is derived from the  $G$ -matrix elements of the Reid potential. The parametrized form of the M3Y interaction from Satchler and Love [23,26] is used for the calculations. Therefore the nuclear and Coulomb potentials of the  $\alpha$ -core system in the DDCM are fully microscopic [22,23].

We now generalize our spherical calculations of the DDCM [16,17] to the deformed case. It is well known that the penetration factor of the  $\alpha$  particle through the Coulomb barrier plays a crucial role in  $\alpha$ -decay calculations. The magnitude of the  $\alpha$ -decay width is mainly determined by the corresponding penetration probability. The polar-angle-dependent penetration probability of  $\alpha$  decay is given by

$$P_\beta = \exp \left[ -2 \int_{R_{\text{in}}(\beta)}^{R_{\text{out}}} \sqrt{\frac{2\mu}{\hbar^2} |Q_\alpha - V_{\text{Total}}(R, \beta)|} dR \right], \quad (8)$$

where  $R_{\text{in}}(\beta)$  and  $R_{\text{out}}$  are two classical turning points defined by the equation  $V_{\text{Total}}(R, \beta) = Q_\alpha$ ,  $\mu$  is the reduced mass of the  $\alpha$ -core system,  $Q_\alpha$  is the experimental  $\alpha$ -decay energy [11,17,30], and  $V_{\text{Total}}$  is the total  $\alpha$ -core potential for which the depth of the nuclear potential is renormalized for all

orientations to ensure a quasi-stationary state by application of the Bohr-Sommerfeld quantization condition [11,17]. It should be noted that the depth of the nuclear potential is not an adjusting parameter and the variation of its value is small for different nuclei [17]. Here the calculation of  $P_\beta$  in each direction is similar to that of previous researches [17] but the complexity and time of computation are much more than those of previous researches. We obtain the total penetration factor  $P$  by averaging  $P_\beta$  in all directions  $P = \frac{1}{2} \int_0^\pi P_\beta \sin(\theta) d\theta$ . This is widely used in both  $\alpha$ -decay and fusion reaction calculations [18,19]. In the DDCM, the  $\alpha$ -decay width has the following expression:

$$\Gamma = P_\alpha F \frac{\hbar^2}{4\mu} \frac{1}{2} \int_0^\pi P_\beta \sin(\theta) d\theta, \quad (9)$$

where  $P_\alpha$  is the preformation probability of the  $\alpha$  particle in the parent nucleus,  $F$  is the normalization factor [11,17], and its value is also obtained by similarly averaging along different orientation angles. The spherical  $\alpha$ -decay width has been applied to spherical  $\alpha$ -decay calculations [10–12,17]. The generalization to the deformed case is an important development on the model and will be useful for future studies. The width is then related to the half-life by the well-known relationship  $T_{1/2} = \hbar \ln 2 / \Gamma$  [11,12,17].

Before we present detailed calculations, it is interesting to illustrate the microscopic double-folding potentials in which the deformation effect is included. In Fig. 1, we plot the nuclear potentials of  $^{236}\text{U}$  for two different orientations  $\beta = 0^\circ$  (red curve) and  $\beta = 90^\circ$  (blue curve). The deformation parameters ( $\beta_2 = 0.207$ ,  $\beta_4 = 0.108$ ) of the daughter nucleus of  $^{236}\text{U}$  are taken from Möller *et al.* [20]. Because the deformation parameters from Möller *et al.* [20] agree well with the magnitude of experimental deformation [21], the values from Möller *et al.* [20] are usually used for calculations of  $\alpha$ -decay half-lives of deformed nuclei [18,19]. Another reason to prefer the values of [20] is that the experimental value of deformation is the absolute value [21] and it cannot differentiate the sign of deformation (i.e., the prolate shape or oblate one). The experimental value of hexadecapole deformation is also

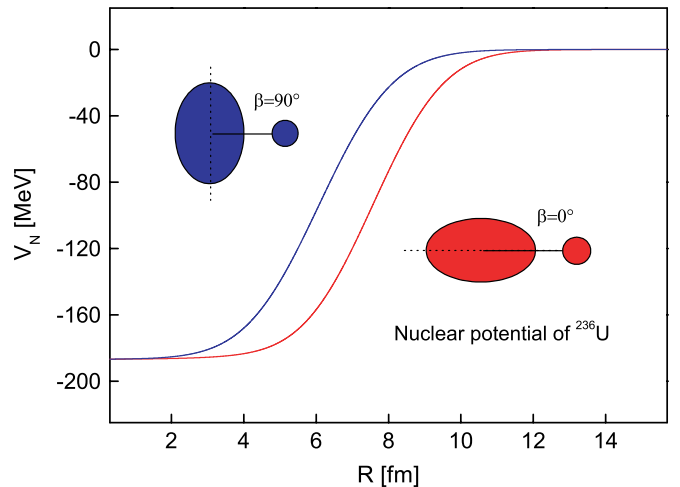


FIG. 1. (Color online) The double-folding nuclear potential of  $^{236}\text{U}$  for two orientations,  $\beta = 0^\circ$  and  $\beta = 90^\circ$ .

rare [21]. The difference between the experimental deformation and that from Möller *et al.* [20] is small and its influence on calculated half-lives is not large.

It is seen from Fig. 1 that the nuclear potentials at  $\beta = 0^\circ$  and at  $\beta = 90^\circ$  are almost the same in both the inner and the outer regions. In the middle region, the shape of the double-folding potentials varies significantly for these two orientations. We can see that the nuclear potential at  $\beta = 0^\circ$  is much deeper than that at  $\beta = 90^\circ$  in the region of 2–12 fm. This is not surprising because there is a large overlap of nuclear density distributions at angle  $\beta = 0^\circ$ . For smaller deformation parameters, the shape of the double-folding nuclear potentials becomes closer for different orientations. Obviously, it is back to that of the spherical case if we take zero-quadrupole and zero-hexadecapole deformations.

In previous studies, we made systematic calculations of  $\alpha$ -decay half-lives by the spherical DDCM [17]. It is quite useful to compare the variation of each term of the decay width between the spherical case and the deformed one. The first term of the decay width [Eq. (9)] is the preformation factor, which is usually assumed to be a constant in  $\alpha$  decay. The normalization factor  $F$  and the penetration factor  $P$  in the decay width are both obtained by the same averaging procedure [Eq. (9)]. Through a detailed analysis, we found that the value of the normalization factor  $F$  remains almost unaffected in the two approximations, but the penetration factor  $P$  varies significantly if the deformation effect is taken into account. This is due to the expression of the penetration factor as an exponential [see Eq. (8)], and its variation is larger than that of a nonexponential function when averaging in all directions. Therefore the penetration factor is more sensitive to the nuclear deformations than are other terms of the decay width. The experimental preformation factor is smaller than 1.0 in both  $\alpha$ -transfer reactions and  $\alpha$  decays [7]. The microscopic calculation also gives a value of  $P_\alpha = 0.3$  for the  $\alpha$  preformation factor of  $^{212}\text{Po}$  [9]. Very interestingly, we have found that the experimental half-lives of all even-even nuclei can be well reproduced by using the same preformation factor  $P_\alpha = 0.38$  in deformed calculations. This is for available experimental data of all even-even nuclei with  $Z = 52$ –104. Its value agrees with both the experimental facts and the microscopic calculations [7–9]. We also note that the preformation factor of the  $\alpha$  cluster is not used in a generalized liquid-drop model (GLDM), which is also a very successful model of half-lives based on a fission approach [15]. The assault frequency is used in GLDM [15].

Now we discuss the calculation of half-lives of favored  $\alpha$  decays in which favored  $\alpha$  decays mean zero angular momentum of an  $\alpha$  particle. This is true for the case of  $\alpha$  decay between the ground states of even-even nuclei [30]. In this communication we restrict our study mainly to the ground-state  $\alpha$  transitions of even-even nuclei ( $Z = 52$ –104) with accurate experimental data. A more comprehensive investigation including the odd- $A$  and odd-odd nuclei will be presented later. In our calculations, we use the experimental  $\alpha$ -decay energies  $Q_\alpha$  [17,30], and the values of the quadrupole and hexadecapole deformations ( $\beta_2, \beta_4$ ), are taken from Ref. [20], correspond to the daughter nucleus. We give both the experimental  $\alpha$ -decay half-lives and theoretical ones for a

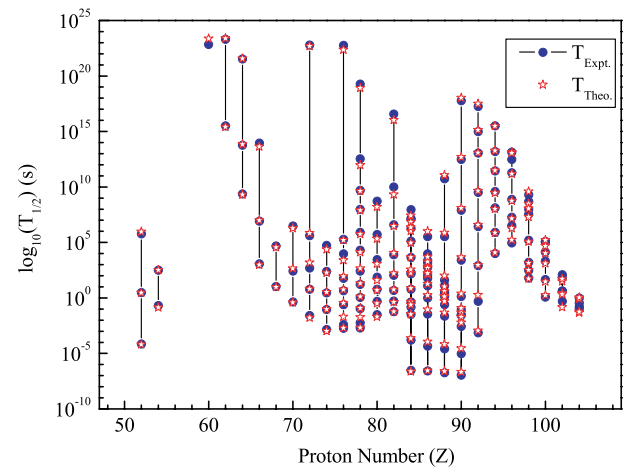


FIG. 2. (Color online) The comparison of experimental  $\alpha$ -decay half-lives and theoretical ones for even-even nuclei ( $Z = 52$ –104).

total of 157 even-even nuclei with  $Z = 52$ –104 for comparison. The variation of  $\alpha$ -decay half-lives with the proton number is drawn in Fig. 2 for isotopic chains. The blue circles denote the experimental data, and the red stars represent the theoretical results. It is known from Fig. 2 that  $\alpha$ -decay half-lives vary in a wide range from  $10^{-8}$  to  $10^{24}$  s. Although the amplitude of the variation of half-lives is as high as  $10^{32}$  times, the theoretical points follow the experimental ones well where they almost coincide with the experimental ones. For the long-lived nuclei ( $T_\alpha > 10^{20}$  s), such as  $^{144}\text{Nd}$ ,  $^{148}\text{Sm}$ ,  $^{152}\text{Gd}$ ,  $^{174}\text{Hf}$ , and  $^{186}\text{Os}$ , the agreement between model and data is very good. Contrary to these nuclei, there are some short-lived  $\alpha$  emitters in the *trans*-Pb region ( $Z = 84$ –90), with  $T_\alpha < 10^{-6}$  s. Our theoretical results are also consistent with the experimental data for these nuclei.

To show the agreement more clearly, we illustrate in Fig. 3 the total agreement between experiment and theory. The X axis is the factor of agreement (FA). When the ratio of experimental half-lives to theoretical ones is between 1/2

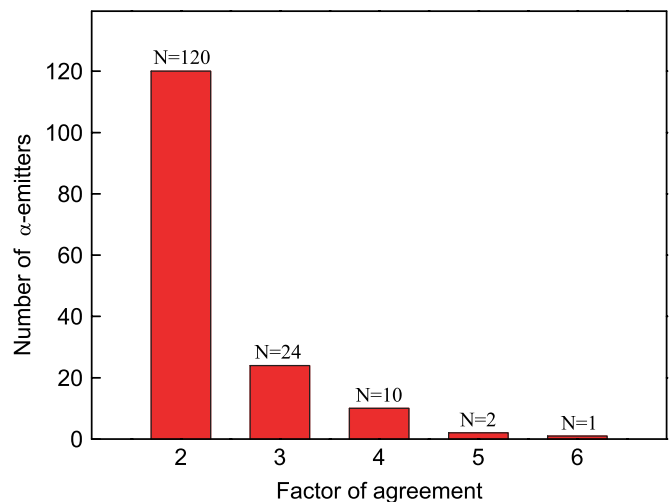


FIG. 3. (Color online) The distribution of the number of  $\alpha$  emitters for different factors of agreement.

TABLE I. Comparison of average and rms deviations of DDCM and GLDM.

Nuclide	Number	Average deviation	rms deviation
Even-even	157 (131)	0.209	0.267(0.35)
Odd-A	231 (192)	0.229	0.285(0.57/0.71)
Odd-odd	79 (50)	0.318	0.435(0.99)

and 2, the FA is defined as  $FA = 2$  because the experimental half-lives are reproduced within a factor of 2 by the DDCM. When the ratio is between  $1/3$  and  $1/2$  or 2 and 3, the FA is  $FA = 3$  and the definitions of other factors are similar to  $FA = 2$  and  $FA = 3$ . The  $Y$  axis is the number of  $\alpha$  emitters in each case. As shown in Fig. 3, we reproduce the half-lives of 120  $\alpha$  emitters within a factor of 2 and 24 within a factor of 3. The FA is larger than 3 for only a few nuclei. The slightly large deviation occurs for the nucleus  $^{210}\text{Po}$ , where the ratio between the experimental half-life and the theoretical one is 5.34  $\{\log_{10}[T(\text{exp})/T(\text{the})] \approx 0.73\}$ . This is due to the influence of the spherical shell closure  $N = 126$  in which the experimental facts also reveal a sudden decrease of the preformation factor of the  $\alpha$  cluster for it [7,8,31]. Here we briefly summarize the overall agreement. The average deviation for the total 157 even-even  $\alpha$  emitters is  $S = \sum_{i=1}^{157} |\log_{10} T_{1/2}^{\text{exp}}(i) - \log_{10} T_{1/2}^{\text{th}}(i)| / 157 = 0.209$ . The logarithm of the average deviation 0.209 corresponds to an absolute deviation of the half-life with a factor of 1.6. This means that the deformed DDCM successfully reproduces the experimental half-lives of even-even nuclei ( $Z = 52-104$ ) within a factor of 2. The spherical version of the DDCM reproduces experimental half-lives within a factor of 2-3 for many medium nuclei and within a factor of 3 for many heavy nuclei [17]. Therefore the deformed version of the DDCM improves greatly the results of spherical calculations.

Before ending this article, let us make a systematic comparison of the deformed DDCM with the GLDM, which also reproduces well the data of  $\alpha$ -decay half-lives [15].

We list the average deviations and root-mean-square (rms) deviations between experimental half-lives and theoretical ones of both even-even nuclei and odd nuclei [32] in Table I. In Table I the second column is the number of  $\alpha$ -emitters of our calculation and the quantity in bracket is that of GLDM [15]. The third column is the average deviation of DDCM and the fourth column is the RMS deviation (in logarithm with a base 10). The quantity in the bracket of column 4 is that of GLDM from Royer [15]. It is seen that both models work very well for the half-lives because the logarithms of deviations 0.3 and 0.6 corresponds to factors of 2 and 4 between experimental half-life and theoretical one, respectively. In future it will be interesting to develop GLDM [15] by including the deformation effect and this can further improve the agreement between the theoretical results and the data. The idea of including deformation in this article is useful for future development of GLDM.

In summary, we present a new version of the DDCM by including the nuclear deformation effect. We calculate the  $\alpha$ -decay half-lives of ground-state transitions of even-even nuclei with  $Z = 52-104$ . The double-folding potentials between the spherical  $\alpha$ -particle and the deformed daughter nucleus are evaluated by the multipole expansion method. The nuclear and Coulomb potentials are fully microscopic and well grounded in physics because the popular M3Y nucleon-nucleon interaction is used for calculations. It is found that the nuclear deformations significantly affect the barrier penetration probabilities and the reason is explained. The theoretical  $\alpha$ -decay half-lives are found to be in excellent agreement with the experimental data. A unified description of  $\alpha$ -decay half-lives of both spherical and deformed nuclei throughout the periodic table is obtained by the deformed version of the DDCM. It is also expected that the deformed version of the DDCM can be used to extract the magnitude of nuclear deformation from very accurate data of  $\alpha$  decays.

This work is supported by the National Natural Science Foundation of China (no. 10535010 and no. 10125521).

- 
- [1] G. Gamov, *Z. Phys.* **51**, 204 (1928).  
[2] E. U. Condon and R. W. Gurney, *Nature (London)* **122**, 439 (1928).  
[3] S. Hofmann and G. Münzenberg, *Rev. Mod. Phys.* **72**, 733 (2000).  
[4] Yu. Ts. Oganessian *et al.*, *Phys. Rev. C* **72**, 034611 (2005).  
[5] J. O. Rasmussen, in *Alpha-, Beta-, and Gamma-Ray Spectroscopy* (North-Holland, Amsterdam, 1965).  
[6] K. Wildermuth and Y. C. Tang, *A Unified Theory of the Nucleus* (Academic, New York, 1977).  
[7] P. E. Hodgson and E. Beták, *Phys. Rep.* **374**, 1 (2003).  
[8] Zhongzhou Ren and Gongou Xu, *Phys. Rev. C* **36**, 456 (1987); *J. Phys. G* **15**, 465 (1989).  
[9] K. Varga, R. G. Lovas, and R. J. Liotta, *Phys. Rev. Lett.* **69**, 37 (1992).  
[10] S. A. Gurvitz and G. Kalbermann, *Phys. Rev. Lett.* **59**, 262 (1987).  
[11] B. Buck, A. C. Merchant, and S. M. Perez, *Phys. Rev. C* **45**, 2247 (1992); *Phys. Rev. Lett.* **72**, 1326 (1994).  
[12] F. Hoyler, P. Mohr, and G. Staudt, *Phys. Rev. C* **50**, 2631 (1994); P. Mohr, *ibid.* **61**, 045802 (2000).  
[13] S. B. Duarte *et al.*, *At. Data Nucl. Data Tables* **80**, 235 (2002).  
[14] B. A. Brown, *Phys. Rev. C* **46**, 811 (1992).  
[15] G. Royer, *J. Phys. G* **26**, 1149 (2000).  
[16] Z. Ren, C. Xu, and Z. Wang, *Phys. Rev. C* **70**, 034304 (2004).  
[17] C. Xu and Z. Ren, *Nucl. Phys.* **A753**, 174 (2005); **A760**, 303 (2005).  
[18] T. L. Stewart, M. W. Kermode, D. J. Beachey, N. Rowley, I. S. Grant, and A. T. Kruppa, *Nucl. Phys.* **A611**, 332 (1996).  
[19] V. Yu. Denisov and H. Ikezoe, *Phys. Rev. C* **72**, 064613 (2005).  
[20] P. Möller, J. R. Nix, W. D. Myers, and W. J. Swiatecki, *At. Data Nucl. Data Tables* **59**, 185 (1995).  
[21] S. Raman, C. H. Malarkey, W. T. Milner, C. W. Nestor Jr., and P. H. Stelson, *At. Data Nucl. Data Tables* **36**, 1 (1987).

- [22] G. F. Bertsch, J. Borysowicz, H. Mcmanus, and W. G. Love, Nucl. Phys. **A284**, 399 (1977).
- [23] G. R. Satchler and W. G. Love, Phys. Rep. **55**, 183 (1979).
- [24] M. J. Rhoades-Brown *et al.*, Z. Phys. A **310**, 287 (1983).
- [25] M. Ismail, A. Y. Ellithi, and F. Salah, Phys. Rev. C **66**, 017601 (2002).
- [26] A. M. Kobos, B. A. Brown, R. Lindsay, and G. R. Satchler, Nucl. Phys. **A425**, 205 (1984).
- [27] J. D. Walecka, *Theoretical Nuclear Physics and Subnuclear Physics* (Oxford University Press, Oxford, 1995), pp. 11–13.
- [28] B. Hahn, D. G. Ravenhall, and R. Hofstadter, Phys. Rev. **101**, 1131 (1956).
- [29] A. Bohr and B. R. Mottelson, *Nuclear Structure* (World Scientific, Singapore, 1998), Vol. 1.
- [30] G. Audi, A. H. Wapstra, and C. Thibault, Nucl. Phys. **A729**, 337 (2003).
- [31] C. Xu and Z. Ren, Commun. Theor. Phys. **42**, 745 (2004).
- [32] C. Xu and Z. Ren, to be submitted.